Available online at www.sciencedirect.com
ScienceDirect
Journal of Magnetic Resonance 184 (2007) 78–84
JMR Journal of Magnetic Resonance
www.elsevier.com/locate/jmr

Distance determination in human ubiquitin by pulsed double electron–electron resonance and double quantum coherence ESR methods

H. Hara [a,*], T. Tenno [b], M. Shirakawa [b]

[a] ESR Division, Bruker Biospin K.K., Ibaraki 305-0051, Japan
[b] Graduate School of Engineering, Kyoto University, Kyoto 606-8502, Japan

Received 8 May 2006; revised 1 September 2006
Available online 13 October 2006

Abstract

Recently, distance measurements by pulsed ESR (electron spin resonance) have been obtained using pulsed DEER (double electron–electron resonance) and DQC (double quantum coherence) in SDSL (site directed spin labeling) proteins. These methods can observe long range dipole interactions (15–80 Å). We applied these methods to human ubiquitin proteins. The distance between the 20th and the 35th cysteine was estimated in doubly spin labeled human ubiquitin. Pulsed DEER requires two microwave sources. However, a phase cycle is not usually required in this method. On the other hand, DQC-ESR at X-band (~9 GHz) can acquire a large echo signal by using pulses of short duration and high power, but this method has an ESEEM (electron spin echo envelope modulation) problem. We used a commercial pulsed ESR spectrometer and compared these two methods.

Keywords: ESR; DEER; DQC-ESR; SDSL; Protein structure; Distance measurement

1. Introduction

Structural analysis of proteins is mainly performed using X-rays or NMR (nuclear magnetic resonance). For X-ray measurements, crystallization of the protein is required and the change in the structure on crystallization is often discussed. Recently, the appearance of high-field NMR has led to an increase in structural analysis by NMR. However, with NMR, measurement of high molecular weight proteins is difficult and a large amount of sample is required. Furthermore, only short distance (less than 0.5 nm) information can be obtained by the detection of residual dipole interactions from NOE (nuclear Overhauser effect) based experiments [1]. On the other hand, for CW-ESR (continuous wave electron spin resonance) measurements in combination with SDSL (site directed spin labeling), distance determination between spin label reagents and molecular motion have been studied [2–4]. SDSL is based on the combination of nitroxide radicals at natural or mutagenically introduced cysteine residues. By measuring these ESR signals, the dipole interaction between spin labeled reagents is determined. ESR is hundreds of times more sensitive than NMR, and ESR requires a much smaller sample concentration (less than 1 mM/l) than NMR. In the CW method, distances are determined by observing changes in the line widths due to dipole interactions. By this method, it is possible to determine distances of up to about 2 nm [5,6].

In recent years, various methods using pulsed ESR have been developed for the structural analysis of proteins, and they have been applied to the photosynthesis system [7–10]. By using pulsed ESR, we can determine long range distances (1.5–8.0 nm) [11,12] and can also estimate distance distributions [13–15]. Recently, by combining pulsed ESR and SDSL, structural analysis of various proteins has been performed [16].

* Corresponding author. Fax: +81 29 858 0322.
E-mail address: Hideyuki.hara@bruker-biospin.jp (H. Hara).

1090-7807/$ - see front matter © 2006 Elsevier Inc. All rights reserved.
doi:10.1016/j.jmr.2006.09.017

Most applications of pulsed ESR use DEER [17–24] (or PELDOR (pulsed electron electron double resonance)) or DQC-ESR [25]. The DEER measurements require a second microwave source to excite another spin species. The spatial distributions and inter-pair interactions of radicals have been studied by Milov et al., using frozen glassy solutions of stabilized radicals and biradicals of the nitroxyl type [5]. The observed signal and the effect of modulation due to dipole interactions are small because the second microwave pulse should excite a part of the spectrum [13]. The advantages of the DEER method are that there are only small ESEEM effects and that phase cycle is not required. In addition, it is possible to measure species with different resonance frequencies, such as the distance between a metal complex and a nitroxide radical or that between metals [9,19,26]. In contrast, the DQC-ESR method detects a double quantum coherence generated by spin–spin interactions. The advantage of this method is that it can excite almost all spins in strong microwave pulses, and, as a result, it has a high sensitivity. However, a 64-step phase operation is necessary to eliminate the unwanted echo and to observe the state of double quantum coherence selectively [16]. Moreover, at X-band measurements, the effect of ESEEM with a peripheral nucleus (hydrogen nucleus) is overlapped on the spectrum. However, if the pulse that excites the spectrum can sufficiently excite the whole spectrum, it is a very effective method.

In this paper, the distance between spin labels in human ubiquitin was determined by using DEER and DQC-ESR with a commercial X-band pulsed ESR spectrometer, and we compared these two methods.

2. Materials and methods

2.1. Sample preparation

For the SDSL sample, mutant human ubiquitin (76 aa) in which Ser20 and Gly35 were mutated to cysteine (S20C, G35C) was used. The plasmid (mutant gene was connected with pET24a vectors) was transferred into *Escherichia coli* cells BL21 (DE3), and was grown at 37 °C in LB medium. It was then induced with 1 mM isopropyl-β,D-thiogalactopyranoside (IPTG), and incubated for 3 h. Cells were sonicated and centrifuged, then incubated for 5 min at 85 °C, and centrifuged again. They were then purified by passing through a cation exchange column and a desalting column (Sephadex G-25). This ubiquitin was buffered with 100 mM K-PO_4 (pH 7.0), a tenfold molar mass of MTSL (1-oxy-2,2,5,5-tetramethylpyrroline-3-yl)methyl methanethiosulfonate was added and the mixture was incubated for 3–4 h at room temperature. Unreacted spin-label regents were removed by a desalting column (Sephadex G-25). Human ubiquitin at a concentration of about 340 μM was buffered with 20 mM K-PO_4, 5 mM KCl and 1 mM EDTA at a pH of 6.8. Thirty weight % glucose was added as a cryoprotectant. About 100 μl of the sample was then loaded into a 5 mm diameter quartz ESR sample tube.

2.2. Experimental

Pulsed ESR measurements were performed on an ELEXSYS E580 X-band FT/CW spectrometer (Bruker BioSpin) equipped with a dielectric resonator (ER4118X-MD5-W1) and a helium gas flow system (CF935, Oxford Instruments). All measurements were performed at 80 K and m.w. pulses 16 ns in duration were used for the 90° pulses for DEER and pulses 8 ns in duration were used for the 90° pulses for the DQC-ESR experiment. All measurements were acquired with the same number of accumulations, 2560 (about 15 min accumulation time, i.e. shots per loop: 40, repetition time: 1 ms, number of scans: 64, data points: about 300. For DQC-ESR experiments, the number of scans is one but it was executed as a 64 phase cycle.). For variable-time DEER measurements, reference and recoupled data, the number of accumulations was 1280. All spectra were taken in single point mode. Obtained spectra were analyzed by using the DEERTrafo program [27].

2.3. Pulse sequence

2.3.1. DEER pulse sequences

Two types of DEER measurements were used, one was a constant-time version [26] and the other was a variable-time version [28]. Four pulse sequences were used for these DEER experiments. Fig. 1 shows the pulse sequences of DEER. The second microwave frequency (ω_B) was supplied by a second microwave source. The pump pulse was set to the maximum of the nitroxide ESR spectrum ($\omega_B = 9.58$ GHz). The observer pulse was set to 60 MHz higher ($\omega_A = 9.64$ GHz) which corresponds to about a 20 Gauss field separation. In this condition, we can detect strong effect in a small echo. All pump pulses were 32 ns in duration. The variable-time experiments could obtain a large signal in a short t because the observed signal intensity is dominated by the spin–spin relaxation time (T_2). The effect of the dipole interaction was obtained by dividing the recoupled trace by the reference trace, so that the SNR (signal to noise ratio) became worse where the signal was small (large t).

2.3.2. DQC-ESR pulse sequences

Two types of DQC-ESR measurements were used, a constant-time version [16] and a variable-time version [29]. Six pulse sequences were used for the DQC-ESR experiments. Fig. 2 shows the pulse sequences of DQC-ESR. 64 step phase cycles were used to eliminate unwanted signals and to observe the state of double quantum coherence selectivity. In the constant-time version, the interval time $t_p + t_2$ is constant. After a time interval $2 * (t_p + t_2 + t_1)$, the change in the echo intensity was observed. This time interval decreases the signal intensity by the spin–spin relaxation time (T_2). In the variable-time version, t_p is constant and only t_2 is changed, so that the signal reduction due to the spin–spin relaxation time is

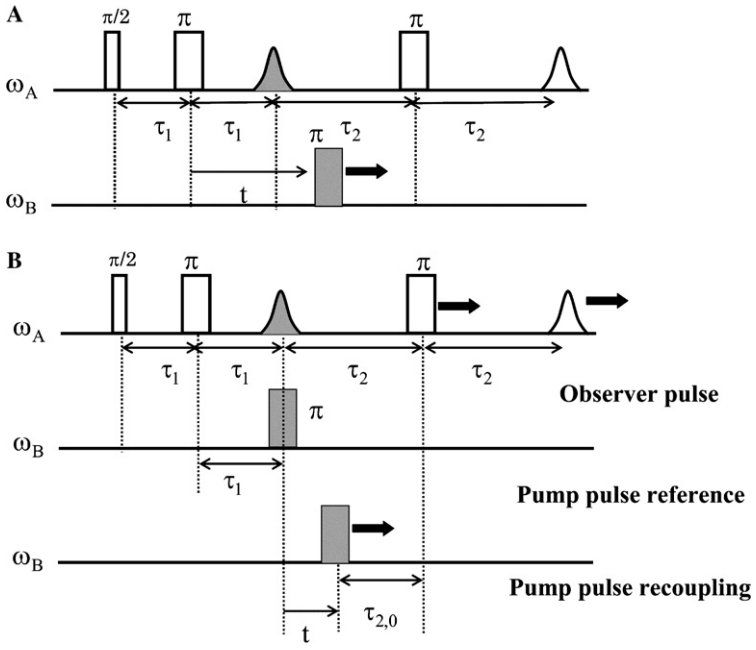

Fig. 1. Pulse sequences for constant-time DEER (A) and variable-time DEER (B). In constant-time DEER, the time t between the second and third pulses of the sequence was increased. In variable-time DEER, the reference spectrum is acquired with an increasing time t but a fixed pump pulse. A recoupled trace is acquired with time t where τ_2 is increased but the delay $\tau_{2.0}$ is kept constant.

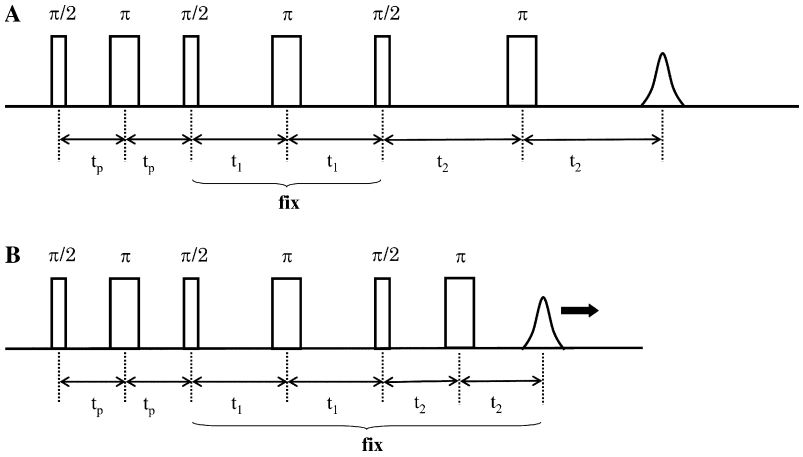

Fig. 2. Pulse sequences for constant-time DQC-ESR (A) and variable-time DQC-ESR (B). In constant-time DQC-ESR, the time t_p was increased and t_2 was decreased. The $t_p + t_2$ was kept constant and the observed echo position was the same. In the variable-time DQC-ESR, the time t_p was increased but t_2 was kept constant. The position of the observed echo changes by t_p.

reduced at the early measurement time. However, it is necessary to consider the influence of the observed dipole interaction on the relaxation time because the position of the detection signal is changing by t_2.

3. Results and discussion

3.1. DEER experiments

The structure of the human ubiquitin and the positions of the MTSL reagent labels at S20C and G35C are shown in Fig. 3. Fig. 4 shows the constant-time (A) and the variable-time (B) DEER spectra as a function of the dipolar evolution time t. Due to intermolecular interactions, the observed spectra contain an exponential decay component [6,26,30]. In the constant-time experiment, SNR is the same in all regions of the spectrum. In the variable-time experiment, the SNR of the time position close to $t = 0$ is better than that at a long t position because the observed echo intensity decreases with t. In our measurements, the proton ESEEM effect was not observed. These characteristics are especially advantageous for short distance determinations. The SNRs of constant- and variable-time versions were 130 and 176, respectively. A Fourier transformed spectrum of the DEER spectrum after subtraction of the exponential decay is shown in Fig. 5. A peak due to the intramolecular

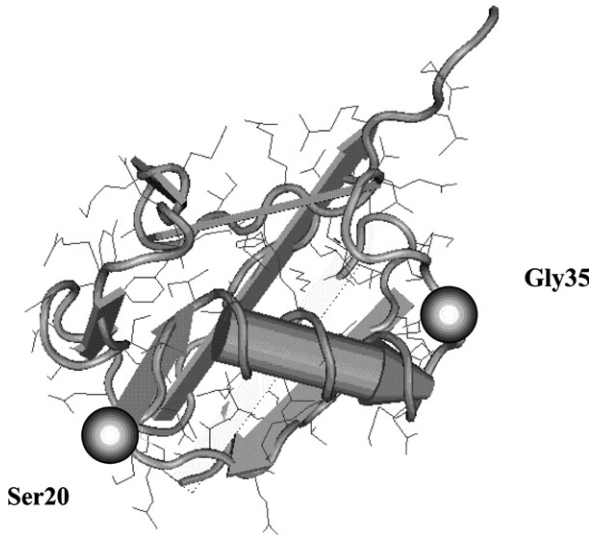

Fig. 3. Structure of human ubiquitin. The spin-labeled mutated sites studied in this work are shown.

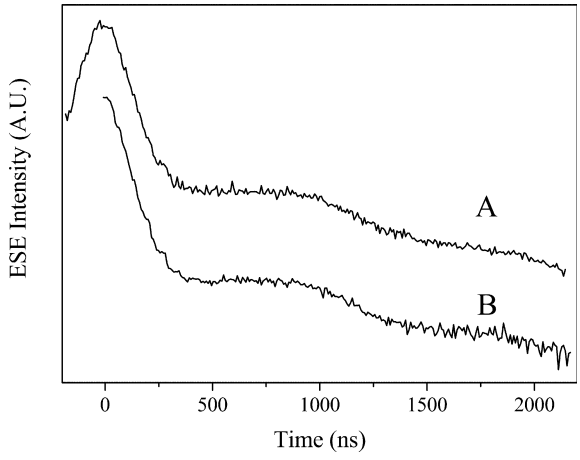

Fig. 4. Constant-time (A) and variable-time (B) DEER spectra. Experimental settings: $\tau_1 = 200$ ns, $\tau_2 = 2200$ ns for constant-time DEER, $\tau_1 = 200$ ns, $\tau_{2.0} = 300$ ns for variable-time DEER.

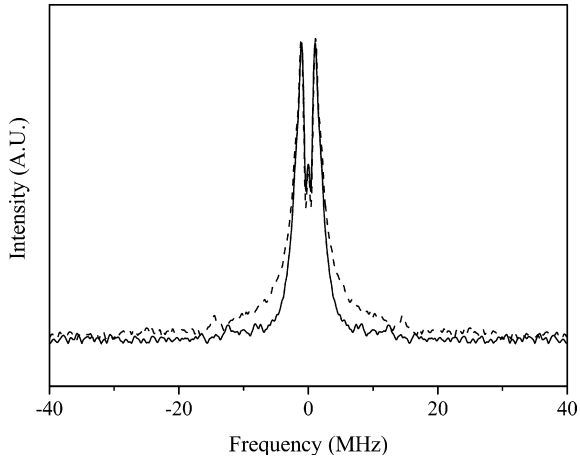

Fig. 5. Fourier transformed spectra of constant-time DEER (solid line) and variable-time DEER (dotted line) after exponential background subtraction.

distribution was observed at 1.1 MHz. There were no other peaks such as from proton ESEEM (~14 MHz). Fig. 6 shows the distances and distance distributions obtained from the constant-time (solid line) and variable-time (dotted line) DEER data after subtraction of the exponential decay using the DEERTrafo program [27]. In both sets of DEER data, the distance and distance distribution were estimated to be $r = 3.55$ nm and $\Delta r = 0.25$ nm, respectively.

3.2. DQC-ESR experiments

Fig. 7 shows the constant-time (A) and variable-time (B) DQC-ESR spectra as a function of the dipolar evolution time; $t_\xi = t_p - t_2$ for the constant-time version and t_p for the variable-time version. In the constant-time version, the obtained spectrum was expanded by a factor of two in the time scale, because that spectrum was obtained as

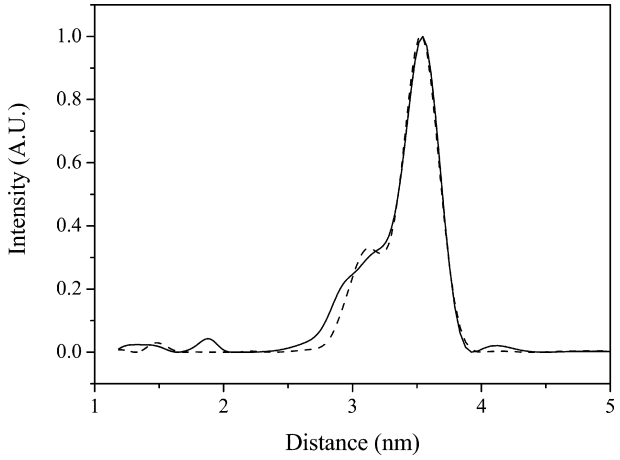

Fig. 6. Distances and distance distributions obtained using constant-time (solid line) and variable-time (dotted line) DEER after exponential background subtraction.

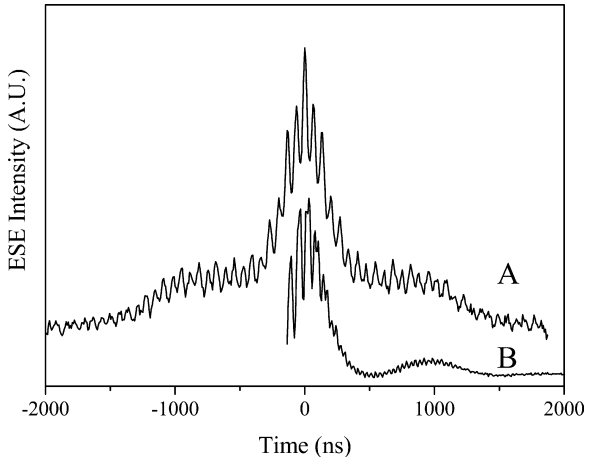

Fig. 7. Constant-time (A) and variable-time (B) DQC-ESR spectra. Experimental settings: $t_p + t_2 = 2200$ ns, $t_1 = 72$ ns for constant-time DQC-ESR, $t_1 = 72$ ns, $t_2 = 200$ ns for variable-time DQC-ESR.

a function of $t_\xi = t_p - t_2$. The t_p was increased and t_2 was decreased simultaneously ($\Delta t_p = -\Delta t_2$) so that the dipolar interaction was observed as a function of $2\Delta t_p$. In both spectra, large modulation due to proton ESEEM was observed. In the variable-time experiment, the effect of the dipolar interaction decreases when the pulse interval t_p becomes long, because of the effect of the spin–spin relaxation time. Despite the effect of the intermolecular interaction being observed by DEER and the constant-time DQC-ESR experiments, the exponential decay due to this intermolecular effect was hardly observed in the DQC-ESR variable-time experiments. This phenomenon was also reported by Bonora et. al. [29]. A Fourier transformed spectrum of the DQC-ESR spectrum after subtraction of the exponential decay is shown in Fig. 8. A peak due to the intramolecular interaction was observed at 1.1 MHz. In the variable-time version, a peak due to proton ESEEM was observed around 14 MHz. The peak was also observed around 28 MHz. This frequency is double the proton ESEEM frequency and also comes from a proton [30]. In the constant-time version, the peaks were observed around 7 and 14 MHz, these values are half those of the frequencies of the variable-time version. In the constant-time version, the obtained spectrum was expanded by a factor of two in the time scale, so that in the frequency scale, the proton ESEEM peaks were observed at half the frequencies. The frequencies of 7, 14, and 28 MHz correspond to 1.9, 1.5 and 1.2 nm, respectively. So if the distance between the spin-labels is in this range, these frequencies will disturb the distance result. Fig. 9 shows the distance and distance distribution obtained from the constant-time (solid line) and the variable-time (dotted line) DQC-ESR data after subtraction of the exponential decay. In both sets of DQC-ESR data, the distance and distance distribution were estimated to be $r = 3.58$ nm and $\Delta r = 0.35$ nm, respectively. In the DQC-ESR data, another distance component was observed at about 1.47 nm. This distance corresponds to the modulation frequency of the proton

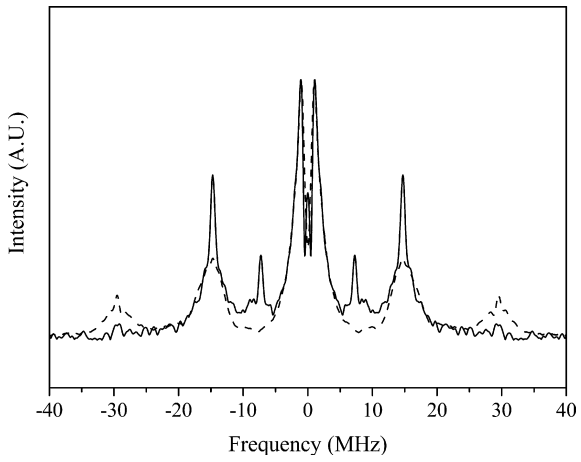

Fig. 8. Fourier transformed spectra of constant-time DQC-ESR (solid line) and variable-time DQC-ESR (dotted line) after exponential background subtraction.

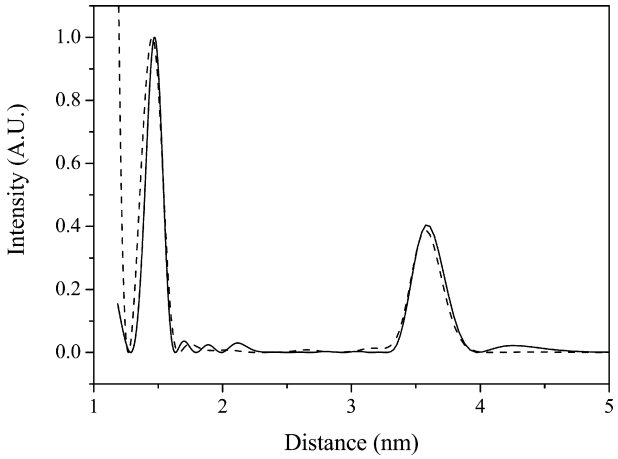

Fig. 9. Distances and distance distributions obtained using constant-time (solid line) and variable-time (dotted line) DQC-ESR after exponential background subtraction.

ESEEM. In X-band, it is difficult to determine a short distance (less than 2 nm) by DQC-ESR. Using high-field ESR, such as Q-band pulse ESR, the proton ESEEM frequency shifts to a higher frequency [26] (about 56 MHz corresponds to 1.0 nm at Q-band) and this ESEEM effect can be eliminated. In X-band, a method to suppress proton ESEEM peaks has been developed [29], but it decreases the SNR.

3.3. Comparison of DEER and DQC-ESR methods

The distances estimated by the DEER and DQC-ESR methods were $r = 3.55$ nm and $r = 3.58$ nm, respectively. According to the 1.8 Å resolution X-ray structural analysis, the distance between the α-carbons for these two labeling sites was estimated to be 2.18 nm [31]. This value differs from our work by about 1.4 nm. In this work, we used MTSL for the spin label reagents. If there is no structural disturbance around the spin label sites the distance between the α-carbons and nitroxide is about ~0.7 nm. In our measurements, the distance distributions were estimated to be about 0.3 nm. Considering the protein structure and size (~8.6 kDa), it is thought that the motion of the protein is small. This means that the observed distribution would come from the motion of the spin label reagent, which means that the labeled sites (α-carbon) are located on outer surface of the protein. If these labeled sites were located to oppositely, the observed distance would lengthen by about 1.4 nm. Taking into account the X-ray structural analysis, this is reasonable because Ser20 and Gly35 are located on the outside of the protein.

Fig. 10 shows the distances and distance distributions observed by constant-time DEER (A) and constant-time DQC-ESR (C). A small difference in the distances and distance distributions was observed between the methods. The DEER seems to show that about 25% of the proteins are in a conformation that places the labels within about 3.0 nm of each other and the other 75% are in a conformation with

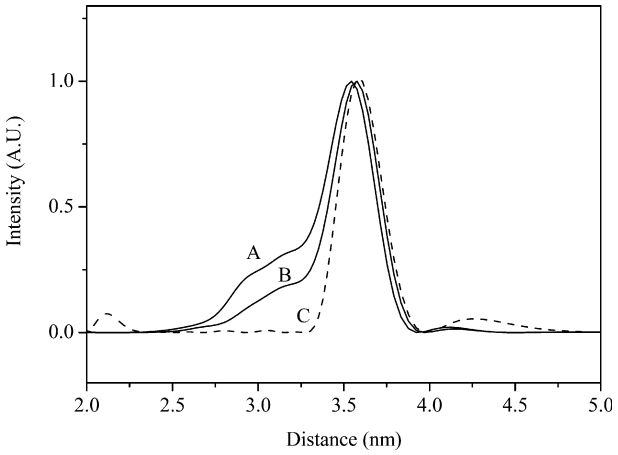

Fig. 10. Distances and distance distributions obtained using constant-time DEER [solid line, (A and B)] and constant-time DQC-ESR [dotted line, (C)] after exponential background subtraction. (A) The pump pulse was set to the maximum of the nitroxide ESR spectrum ($\omega_B = 9.58$ GHz) and the observer pulse was set to 60 MHz higher ($\omega_A = 9.64$ GHz). (B) The observer pulse was set to the maximum of the nitroxide ESR spectrum ($\omega_B = 9.64$ GHz) and the pump pulse was set to 60 MHz higher ($\omega_A = 9.70$ GHz).

about 3.55 nm between labels. On the other hand, the DQC-ESR shows longer distance configuration about 3.58 nm. In the DQC-ESR experiments, we used an 8 ns duration for a 90° pulse, corresponding to the 125 MHz (~45 Gauss) excited region. The spectrum of the observed nitroxide radical was about 200 MHz (~70 Gauss). For the DQC-ESR measurements, it is desirable that all spectral regions are excited by the m.w. pulse, but this was restricted by the output power of the m.w. TWT amplifier. On the other hand, for DEER measurements, it is necessary to adjust the m.w. frequency and pulse width to avoid overlapping of this range of excitation. Overlapping of the excitation region induces the proton ESEEM effect in DEER spectra. In DEER experiments, the difference in frequency was set to 60 MHz from the peak intensity and an observer pulse ($\omega_A = 9.64$ GHz) 16 ns in duration for a 90° pulse and pump pulses ($\omega_B = 9.58$ GHz) 32 ns in duration were used (Fig. 10(A)). The observed nitroxide radical shows an anisotropic spectrum and it is necessary to consider an anisotropic effect because only a part of the spectrum is excited in DEER measurements, while the whole spectrum is excited in DQC-ESR. To confirm this orientation selection in DEER experiments, we changed the observer and pump pulses position. The observer pulse was set to the maximum of the nitroxide ESR spectrum ($\omega_B = 9.64$ GHz) and the pump pulse was set to 60 MHz higher ($\omega_A = 9.70$ GHz). In this condition, we can detect small effect in a large echo. The observed modulation depth was almost same as above experiments (data not shown). However a small difference in the distances and distance distributions was observed (Fig. 10(B)). The short distance configuration about 3.0 nm was decreased and the conformation about 3.55 nm shifted toward longer distance. On the other hand, the DQC-ESR method is practically free from orientation selection. This result indicates that the difference in the distance and distribution comes from the orientation selection of the nitroxide radical. It is thought that the DQC-ESR method shows the more accurate distance between the spin labels.

In a comparison between DEER and DQC-ESR methods, DEER methods are advantageous for determining short distances because they have no ESEEM effect. Furthermore, by using variable-time DEER, the SNR at a short t was improved. At X-band, the DQC-ESR methods are disadvantageous for short distance determinations because of the ESEEM effect. However, for longer distance determinations, variable-time DQC-ESR is especially advantageous. In the variable-time DQC-ESR, the proton ESEEM effect becomes weak at long t_p values and the effects of intermolecular interactions are suppressed. This suppression of intermolecular interactions is very advantageous in long distance determinations because this intermolecular interaction has a greater influence in long distance determinations, though further discussion on this phenomena is required.

4. Conclusion

In this work, we measured human ubiquitin protein by DEER and DQC-ESR at X-band using a commercial FT-ESR spectrometer. The distance between the 20th and 35th cysteines was estimated as 3.55 nm by DEER and 3.58 nm by DQC-ESR. DEER is advantageous for determining short distances. Variable-time DEER can achieve a better SNR than the constant-time version [28]. The experimental setup of DEER methods is easy because DEER methods do not need a phase cycle. DQC-ESR can achieve a strong signal intensity but has an ESEEM effect [16,29]. It needs a complex phase cycle [16] and precise pulse angles. In short distance measurements (<2 nm), we must carefully distinguish this ESEEM effect. However, with variable-time DQC-ESR, the intermolecular interaction effect was reduced [29] and the intramolecular interaction is emphasized. This is especially advantageous for long distance determinations.

This experiment on distance determination with spin labels shows that the utility of ESR methods can be increased by the selection of proper methods.

References

[1] H. Bohr, S. Brunak, Protein Folds: A Distance-Based Approach, CRC Press, Boca Raton, Florida, 1996.
[2] W.L. Hubbell, C. Altenbach, Curr. Opin. Struct. Biol. 4 (1994) 566–573.
[3] L.J. Berliner, S.S. Eaton, G.R. Eaton (Eds.), Biological Magnetic Resonance, vol. 19, Plenum, New York, 2000.
[4] H.J. Steinhoff, B. Suess, Methods 29 (2003) 188–195.
[5] A.D. Milov, K.M. Salikhov, M.D. Shirov, Fiz. Tverd. Tela (Leningrad) 23 (1981) 957–982.
[6] A.D. Milov, A.B. Ponomarev, Yu. D. Tsvetkov, Chem. Phys. Lett. 110 (1984) 67–72.
[7] H. Hara, A. Kawamori, Appl. Magn. Reson. 13 (1997) 241–257.

[8] H. Hara, S.A. Dzuba, A. Kawamori, K. Akabori, T. Tomo, K. Satoh, M. Iwaki, S. Itoh, Biocim. Biophys. Acta 1322 (1997) 77–85.
[9] H. Hara, A. Kawamori, A.V. Astashkin, T. Ono, Biocim. Biophys. Acta 1276 (1996) 140–146.
[10] A.V. Astashkin, H. Hara, A. Kawamori, Biochim. Biophys. Acta. 1363 (1998) 187–198.
[11] L.V. Kulik, Yu.A. Grishin, S.A. Dzuba, I.A. Grigoryev, S.V. Klyatskaya, S.F. Vasilevsky, Yu.D. Tsvetkov, J. Magn. Reson. 157 (2002) 61–68.
[12] A.A. Dubinskii, Yu.A. Grishin, A.N. Savitsky, K. Möbius, Appl. Magn. Reson. 22 (2002) 369–386.
[13] G. Jeschke, A. Koch, U. Jonas, A. Godt, J. Magn. Reson. 155 (2001) 72–82.
[14] G. Jeschke, Chem. Phys. Chem 3 (2002) 927–932.
[15] G. Jeschke, G. Panek, A. Godt, A. Bender, H. Paulsen, Appl. Magn. Reson. 26 (2004) 223–224.
[16] P.P. Borbat, H.S. Mchaourab, J.H. Freed, J. Am. Chem. Soc. 124 (2002) 5304–5314.
[17] E. Narr, A. Godt, G. Jeschke, Chem. Int. Ed. 41 (2002) 3907–3910.
[18] G. Jeschke, Macromil. Rapid. Commun. 23 (2002) 227–246.
[19] I.M.C. vanAmsterdam, M. Ubbink, G.W. Canters, M. Huber, Angew. Chem. Int. Ed. 42 (2003) 62–64.
[20] M. Bennati, A. Weber, J. Antonic, D.L. Perlstein, J. Robblee, J. Stubbe, J. Am. Chem. Soc. 125 (2003) 14988–14989.
[21] A.G. Maryasov, Y.D. Tsvetkov, J. Raap, Appl. Magn. Reson. 14 (1998) 101–113.
[22] A.D. Milov, A.G. Maryasov, Y.D. Tsvetkov, Appl. Magn. Reson. 15 (1998) 107–143.
[23] A.D. Milov, Y.D. Tsvetkov, Appl. Magn. Reson. 12 (1997) 495–504.
[24] A.D. Milov, Y.D. Tsvetkov, F. Formaggio, M. Crisma, C. Toniolo, J. Raap, J. Am. Chem. Soc. 123 (2001) 3784–3789.
[25] P.P. Borbat, H.S. Mchaourab, J.H. Freed, J. Am. Chem. Soc. 124 (2002) 5304–5314.
[26] M. Pannier, S. Veit, A. Godt, G. Jeschke, H.W. Spiess, J. Magn. Reson. 142 (2000) 331–340.
[27] http://www.mpip-mainz.mpg.de/~jeschke/distance.html.
[28] G. Jeschke, A. Bender, H. Paulsen, H. Zimmermann, A. Godt, J. Magn. Reson. 169 (2004) 1–12.
[29] M. Bonora, J. Becker, S. Saxena, J. Magn. Reson. 170 (2004) 278–283.
[30] S.A. Dikanov, Y.D. Tsvetkov, Electron Spin Echo Envelope Modulation (ESEEM) Spectroscopy, CRC Press, Boca Raton, FL, 1992.
[31] S. Vijay-Kumar, C.E. Bugg, W.J. Cook, J. Mol. Biol. 194 (1987) 531–544.